Development 137, 1515-1522 (2010) doi:10.1242/dev.044545
© 2010. Published by The Company of Biologists Ltd

The oscillation of Notch activation, but not its boundary, is required for somite border formation and rostral-caudal patterning within a somite

Masayuki Oginuma[1,2,*], Yu Takahashi[3,*], Satoshi Kitajima[3], Makoto Kiso[2], Jun Kanno[3], Akatsuki Kimura[1,4] and Yumiko Saga[1,2,†]

SUMMARY

Notch signaling exerts multiple roles during different steps of mouse somitogenesis. We have previously shown that segmental boundaries are formed at the interface of the Notch activity boundary, suggesting the importance of the Notch on/off state for boundary formation. However, a recent study has shown that mouse embryos expressing Notch-intracellular domain (NICD) throughout the presomitic mesoderm (PSM) can still form more than ten somites, indicating that the NICD on/off state is dispensable for boundary formation. To clarify this discrepancy in our current study, we created a transgenic mouse lacking NICD boundaries in the anterior PSM but retaining Notch signal oscillation in the posterior PSM by manipulating the expression pattern of a Notch modulator, lunatic fringe. In this mouse, clearly segmented somites are continuously generated, indicating that the NICD on/off state is unnecessary for somite boundary formation. Surprisingly, this mouse also showed a normal rostral-caudal compartment within a somite, conferred by a normal Mesp2 expression pattern with a rostral-caudal gradient. To explore the establishment of normal Mesp2 expression, we performed computer simulations, which revealed that oscillating Notch signaling induces not only the periodic activation of *Mesp2* but also a rostral-caudal gradient of Mesp2 in the absence of striped Notch activity in the anterior PSM. In conclusion, we propose a novel function of Notch signaling, in which a progressive oscillating wave of Notch activity is translated into the rostral-caudal polarity of a somite by regulating *Mesp2* expression in the anterior PSM. This indicates that the initial somite pattern can be defined as a direct output of the segmentation clock.

KEY WORDS: Notch signaling, Hes7, Mesp2, Segmentation clock, Presomitic mesoderm, Lunatic fringe, Somitogenesis

INTRODUCTION

The periodicity of the segmented somites is established in the posterior presomitic mesoderm (PSM) via the function of a so-called molecular clock, which is based on complex gene regulatory networks under the control of three major signaling pathways: Notch, Fgf and Wnt (Dequeant et al., 2006; Dequeant and Pourquie, 2008). Among these pathways, Fgf and Wnt are implicated in the maintenance of immature PSM cells (Aulehla et al., 2003; Aulehla et al., 2008; Wahl et al., 2007; Delfini et al., 2005; Niwa et al., 2007), whereas Notch signaling might be directly involved in the generation of periodicity (Oginuma et al., 2008; Yasuhiko et al., 2006; Takahashi et al., 2000; Takahashi et al., 2003). In mice, Notch signal oscillations are produced by the suppressive function of the glycosyltransferase lunatic fringe (Lfng) as the levels of activated Notch1 (cleaved form of the Notch1 intracellular domain, referred to as cNICD hereafter) are upregulated in the *Lfng*-null mouse embryo (Morimoto et al., 2005). The expression of *Lfng* exhibits a biphasic pattern involving oscillation in the posterior PSM and a stabilized striped pattern in the anterior PSM (Aulehla and Johnson, 1999; McGrew et al., 1998; Morales et al., 2002; Cole et al., 2002). The oscillatory expression of *Lfng* is positively regulated by Notch signaling as it is greatly downregulated in *Dll1*-null mice, whereas it is negatively regulated by Hes7 as revealed by its upregulation in *Hes7*-null embryos (Barrantes et al., 1999; Bessho et al., 2003; Morales et al., 2002). The stabilized expression of *Lfng* is under the control of the Mesp2 transcription factor and stabilization does not occur in the absence of Mesp2 (Morimoto et al., 2005). In the absence of Lfng, no clear segmental border is defined and the rostral-caudal (R-C) compartmentalization within a somite is randomized (Zhang and Gridley, 1998; Evrard et al., 1998).

In the anterior PSM, the Mesp2 transcription factor plays an important role in the creation of a cNICD on/off state that corresponds to the future segmental boundary via the activation of Lfng transcription (Morimoto et al., 2005). This suggests that the Notch on/off state is important for boundary formation. However, a recent study has shown that mouse embryos expressing Notch activity throughout the PSM still show the ability to form more than ten somites, indicating that the Notch on/off state is dispensable for boundary formation (Feller et al., 2008). By contrast, however, other studies have reported that transgenic mice expressing *Lfng* only in the anterior PSM show normal segmental border formation after embryonic day 10.5 (E10.5), suggesting that the Notch on-off state generated in the anterior PSM is sufficient to create a somite boundary at least in the later stage embryos (Shifley et al., 2008; Stauber et al., 2009).

To resolve this discrepancy, we have, in our current study, generated a mouse that lacks the anterior striped Lfng expression pattern, but at the same time retains oscillating Lfng activity in the

[1]Department of Genetics, SOKENDAI, 1111 Yata, Mishima, Shizuoka 411-8540, Japan. [2]Division of Mammalian Development, National Institute of Genetics, Yata 1111, Mishima 411-8540, Japan. [3]Division of Cellular and Molecular Toxicology, National Institute of Health Sciences, 1-18-1 Kamiyoga, Setagaya-ku, Tokyo 158-8501, Japan. [4]Cell Architecture Laboratory, National Institute of Genetics, Yata 1111, Mishima 411-8540, Japan.

*These authors contributed equally to this work
†Author for correspondence (ysaga@lab.nig.ac.jp)

Accepted 17 February 2010

posterior PSM. The resulting transgenic mouse shows no clear cNICD on/off state in the anterior PSM. Nevertheless, this mouse exhibits normal boundary formation, indicating that the cNICD boundary is dispensable for somite formation. In addition, our transgenic mouse shows normal R-C patterning within a somite. Further analyses by computer simulation have led us to conclude that Notch signaling oscillation functions as an output signal that is both required and sufficient to establish the *Mesp2* expression pattern needed for normal somitogenesis.

MATERIALS AND METHODS

Animals

The wild-type mice used in this study were the MCH strain (a closed colony established at CLEA, Japan). The *Lfng*-null (Evrard et al., 1998), *Mesp2*-null (*Mesp2*$^{MCM/+}$) (Takahashi et al., 2007) and *Mesp2-lacZ* (*Mesp2*$^{lacZ/+}$) (Takahashi et al., 2000) mouse lines are maintained in the animal facility of the National Institute of Genetics and National Institute of Health Sciences, Japan.

Gene targeting strategy to generate the *Mesp2*^{Lfng} allele

The knock-in strategy used to target the *Mesp2* locus is largely similar to our previously described method (Takahashi et al., 2000), except that *Lfng* cDNA was inserted. The *pgk-neo* cassette flanked by a *lox* sequence was removed by crossing with *CAG-Cre* mice (Sakai and Miyazaki, 1997).

Generation of the *Hes7-Lfng* transgenic mice

We used a 12 kb *Hes7* gene cassette comprising 5 kb of upstream sequence and all of the exons and introns, as this construct had previously been confirmed to be sufficient to reproduce the endogenous *Hes7* oscillation pattern when inserted in-frame at the translational start site (Kageyama et al., personal communications). We generated the construct *Lfng IRES-EGFP*, in which *IRES* (internal ribosomal entry site)-*EGFP* (enhanced GFP) was fused to the 3′ end of *Lfng* cDNA, and inserted this construct into the *Hes7*-translational initiation site. The resulting DNA was digested with restriction enzymes to remove vector sequences and gel purified. Transgenic mice were generated by microinjection of this construct into fertilized eggs, which were then transferred into the oviducts of pseudopregnant foster females.

In situ hybridization, immunohistochemistry, histology and skeletal preparations

The methods used for wholemount in situ hybridization, section in situ hybridization, immunohistochemistry, histology and skeletal preparation by Alcian Blue/Alizarin Red staining are described in our previous reports (Morimoto et al., 2005; Oginuma et al., 2008; Takahashi et al., 2000). The cNICD signal was detected by immunohistochemistry using anti-cleaved NICD (Val1744; 1:500; Cell Signaling Technology). Probes were prepared also as described previously: *Mesp2* exon-intron (Oginuma et al., 2008), *Mesp2* (Takahashi et al., 2000) and *Lfng* (Evrard et al., 1998). The *GFP* cRNA probe was prepared by PCR-amplification of *GFP* cDNA.

Computer simulation

Our computer simulation model is based on the previous mathematical description of a clock-and-wavefront model constructed by J. Lewis (Palmeirim et al., 1997). By using the basic oscillating function in the Lewis model, we modeled the activity of cNICD, n, at given time, t, and anteroposterior position, x, as:

$$n(x,t)=\left[1-\cos\left\{2\pi\int_0^t\frac{1}{1+e^{(x+t)/2}}dt\right\}\right]/2\,.$$

For the control simulation with constant activity of cNICD, the cNICD activity, n, was set to 0.3. For the simulation with oscillating cNICD without wave, n was formulated as $n(x,t)=\{1-\cos(\pi t)\}/2$. The activity of Fgf8 is known to gradually decrease from posterior to anterior, and also according to the time elapsed. These features of Fgf8 fit well with the formulation of the clock cycling rate in the Lewis model and, thus, we calculated the activity of Fgf8, f, using the formula $f(x,t)=1/(1+e^{(x+t)/2})$.

We next added the regulation of Mesp2 and Tbx6 expression to the model. As cNICD and Fgf8 play positive and negative roles for *Mesp2* expression, respectively, we assumed that the increase of *Mesp2* expression occurs when the cNICD activity, n, exceeds that of Fgf8, f, with the amount dependent on n–f. Tbx6 (b) is also required for *Mesp2* expression. We thus modeled the *Mesp2* mRNA expression, m, and Mesp2 protein expression, p, as:

$$m(x,t+\Delta t)=m(x,t)+S_m\times\frac{[\{n(x,t)-f(x,t)\}/K_n]^{H_n}}{1+[\{n(x,t)-f(x,t)\}/K_n]^{H_n}}\times\frac{\{b(x,t)/K_b\}^{H_b}}{1+\{b(x,t)/K_b\}^{H_b}}-D_m\times m(x,t)\,,$$

$$p(x,t+\Delta t)=p(x,t)+S_p\times m(x,t-T)-D_p\times p(x,t)\,,$$

with the initial condition $m(x,0)=0$, and $p(x,0)=0$. The degradation of Tbx6 is dependent on Mesp2 (Oginuma et al., 2008). We introduced a hypothetical molecule, z, that is expressed depending on Mesp2 and degrades Tbx6 by interacting with it. The expression of Tbx6 (b) and the Tbx6 degrading molecule (z) were modeled as:

$$z(x,t+\Delta t)=z(x,t)+S_z\times\frac{\{p(x,t-T)/K_p\}^{H_p}}{1+\{p(x,t-T)/K_p\}^{H_p}}-D_z\times z(x,t)\,,$$

$$b(x,t+\Delta t)=b(x,t)-D_b\times\{b(x,t)\}^{Bb}\times\{z(x,t)\}^{Bz}\,,$$

with the initial condition $z(x,0)=0$, and $b(x,0)=1.0$.

These formulas were implemented using C language. The activities of cNICD (n), Fgf8 (f), Mesp2 (m and p), Tbx6-regulator (z) and Tbx6 (b) were calculated over the ranges $-12.5\leq x\leq -2.5$ and $0\leq t\leq 20$. The calculations were conducted discretely with a single unit of x (Δx) of 1/10 and t (Δt) of 1/10. The parameter values we used are shown in Table S1 in the supplementary material. We also introduced time delay, $T=2\Delta t$, for protein expression (Lewis, 2003), which did not affect the results much.

RESULTS

Dissection of the *Lfng* expression pattern in the PSM

To examine the significance of the Notch on/off state during boundary formation, we focused on *Lfng* expression, which exhibits a biphasic pattern involving oscillation in the posterior PSM and a stabilized striped pattern in the anterior PSM (Aulehla and Johnson, 1999; Cole et al., 2002; McGrew et al., 1998; Morales et al., 2002). Each of these two patterns is implicated in the generation of the corresponding Notch activity profile via negative regulation. To induce only the oscillatory expression of *Lfng*, we utilized the *Hes7* transcriptional regulatory unit as the oscillation of *Lfng* and *Hes7* is regulated by similar factors, i.e. positively by Notch signaling and negatively by Hes7 protein. As shown in Fig. 1, these two transcripts show similar expression patterns in the oscillation phase. Both signals manifest a waved pattern within the Tbx6 expression domain from phase I to phase III (Fig. 1A-L). However, in phases I-II, *Hes7* expression is lost from the anterior domain (Fig. 1G-J), whereas that of *Lfng* persists for a longer period in the anterior PSM and forms a clear stripe (Fig. 1A-D,M,O). It should also be noted that the anterior *Lfng* expression domain was found to merge with that of the Mesp2 protein (Fig. 1N,P), the expression of which is restricted to the anterior PSM. This is not unexpected as *Lfng* expression is induced by Mesp2 in the anterior PSM and creates the Notch on/off state (Morimoto et al., 2005). Taken together, we concluded from these data that the *Lfng* expression pattern can be reproduced by two distinct regulatory systems – the *Hes7* promoter-enhancer and the *Mesp2* regulatory system – and this enabled us to further investigate the significance of Notch activities.

DEVELOPMENT

The cNICD on/off state is not required for somite boundary formation

To further elucidate the functional significance of the oscillatory cNICD in the posterior PSM and that of the cNICD on/off state in the anterior PSM, we generated a transgenic mouse line by inserting *Lfng* cDNA flanked with *IRES-EGFP* under the control of the Hes7 promoter (see Fig. S1A in the supplementary material). As expected, the expression pattern of this transgene, examined by in situ hybridization using *EGFP* as a probe, was found to be very similar to that of endogenous *Hes7* and *Lfng* except for the lack of anterior striped expression (see Fig. S1B-D in the supplementary material). We then introduced this transgene into the *Lfng*-null genetic background to establish the *Hes7>Lfng/Lfng*$^{-/-}$ mouse line and examined the expression pattern of exogenous *Lfng* and cNICD expression in the absence of endogenous *Lfng* expression (i.e. an *Lfng*-null background). In wild-type embryos, *Lfng* and cNICD showed biphasic patterns, these being oscillation in the posterior PSM and stabilization in the anterior PSM, whereas cNICD oscillation was barely detectable and a constant level of cNICD could be observed through the entire PSM in the absence of *Lfng*, as reported previously (Morimoto et al., 2005). In the *Hes7>Lfng/Lfng*$^{-/-}$ embryo, however, we observed the recovery of cNICD oscillation in the posterior PSM, which overlapped with *Lfng* expression (Fig. 2A-F), clearly indicating that the *Lfng* transgene was functionally active in these embryos. In addition, we previously showed that cNICD and Mesp2 generate a clear boundary in the anterior PSM, which demarcates the presumptive segmental border in phase-II embryos (Morimoto et al., 2005) (Fig. 2G-I). In the absence of *Lfng*, this clear border between cNICD and Mesp2 was not generated and a merged pattern was instead observed

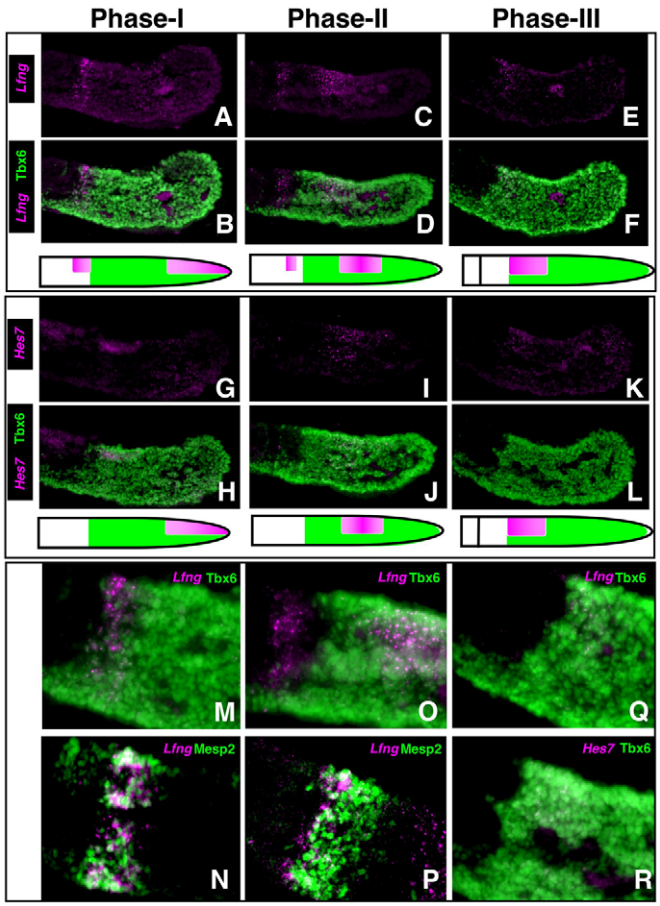

Fig. 1. Comparison of the *Hes7* and *Lfng* expression patterns. In situ hybridization analysis of the spatiotemporal changes in the *Lfng* (**A-F**) and *Hes7* (**G-L**) transcription patterns during somitogenesis by double staining for the Tbx6 protein as the reference point. The stained sections shown in the vertical rows are derived from a single embryo. The phase was defined by the location of the *Hes7* and *Lfng* transcripts and the waves of oscillating *Hes7* and *Lfng* were initiated at the posterior PSM (Phase I). The oscillating wave then moves to the intermediate PSM (Phase II) and reaches the anterior PSM (Phase III). (**M**,**O**,**Q**,**R**) Magnified images of B, D, F and L, respectively. Phase I and Phase II sections were also subjected to double staining for *Lfng* mRNA and Mesp2 (**N**,**P**).

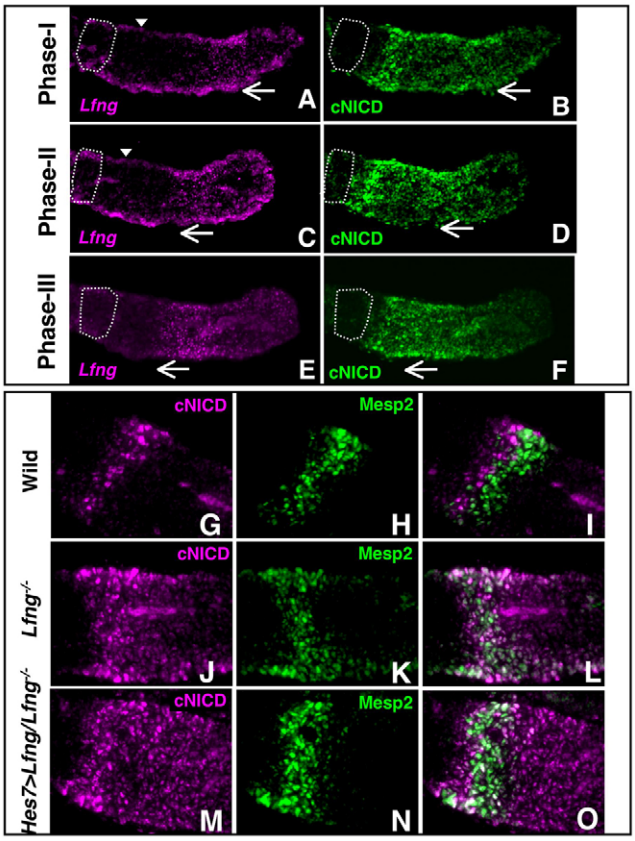

Fig. 2. *Hes7>Lfng/Lfng*$^{-/-}$ mice show cNICD oscillation in the posterior PSM but do not form a cNICD boundary in the anterior PSM. (**A-F**) The patterns of *Lfng* mRNA (A,C,E) and cNICD (B,D,F) expression were revealed in each channel by double staining of these signals using single embryos of *Hes7>Lfng/Lfng*$^{-/-}$ mice at three different phases, I-III, respectively. *Lfng* expression shows a traveling wave (arrow) but no stabilized stripe (arrowheads, A,C). The first somite is indicated by a white dotted line. The wave of oscillating cNICD is initiated at the posterior PSM (B; Phase I; *n*=3), moves to the intermediate PSM (D; Phase II; *n*=4) and eventually reaches the anterior PSM (F; Phase III; *n*=3). (**G-O**) The relationship between cNICD and Mesp2 in Phase II was compared among wild-type (G-I), *Lfng*$^{-/-}$ (J-L) and *Hes7>Lfng/Lfng*$^{-/-}$ (M-O) embryos by double staining. Single channels for cNICD (G,J,M) and Mesp2 (H,K,N), and merged images of both (I,L,O), are shown. In the wild-type embryos, cNICD and Mesp2 generate a clear boundary (I). *Lfng*$^{-/-}$ and *Hes7>Lfng/Lfng*$^{-/-}$ mice, however, do not show a clear segregation between cNICD and Mesp2 (L,O).

(Fig. 2J-L). In the *Hes7>Lfng/Lfng*$^{-/-}$ embryo, as expected by the lack of Lfng expression in the anterior PSM, we did not detect segregation between the cNICD and Mesp2 domains (Fig. 2M-O). *Lfng*$^{-/-}$ embryos did not show clear somite boundaries, although incomplete somites did appear to be formed (see Fig. S2 in the supplementary material), as also suggested previously (Evrard et al., 1998; Zhang and Gridley, 1998). Very surprisingly, however, *Hes7>Lfng/Lfng*$^{-/-}$ embryos showed clearly segmented somites (Fig. 3A-C). This strongly indicates that the oscillatory expression of cNICD mediated via oscillating Lfng is sufficient to provide the conditions for normal somitogenesis to occur and that the cNICD boundary in the anterior PSM is not required for this process.

Recently, we and others have suggested that the Mesp2 downstream events, such as the activation of ephrin-EphA4 signaling and the formation of a Tbx6 protein boundary, were more important for segmental border formation (Watanabe et al., 2009; Oginuma et al., 2008; Nakajima et al., 2006). In *Lfng*$^{-/-}$ embryos, the expression of *EphA4* and the Tbx6 protein boundary were found to be diffuse or randomized (Fig. 3E,J-L), whereas in *Hes7>Lfng/Lfng*$^{-/-}$ embryos, these expression patterns appeared to be normal (Fig. 3F,M-O), i.e. similar to those in wild-type embryos (Fig. 3D,G-I). Taken together, our current findings show that the cNICD boundary is dispensable, but that the Mesp2 boundary might be required, for the creation of the segmental border through the regulation of downstream genes.

R-C polarity is completely recovered in *Hes7>Lfng/Lfng*$^{-/-}$ embryos

We next further examined the morphological features of the *Hes7>Lfng/Lfng*$^{-/-}$ embryo. Surprisingly, these transgenic embryos showed a completely normal skeletal system, with segmented vertebra and ribs (Fig. 4A-C). Furthermore, the expression pattern of *Uncx4.1*, a caudal marker of R-C polarity (Fig. 4D), was fully recovered in the *Hes7>Lfng/Lfng*$^{-/-}$ embryo (Fig. 4F), which contrasts with the randomized pattern we observed in the *Lfng*$^{-/-}$ embryo (Fig. 4E). These results suggest that the cNICD boundary in

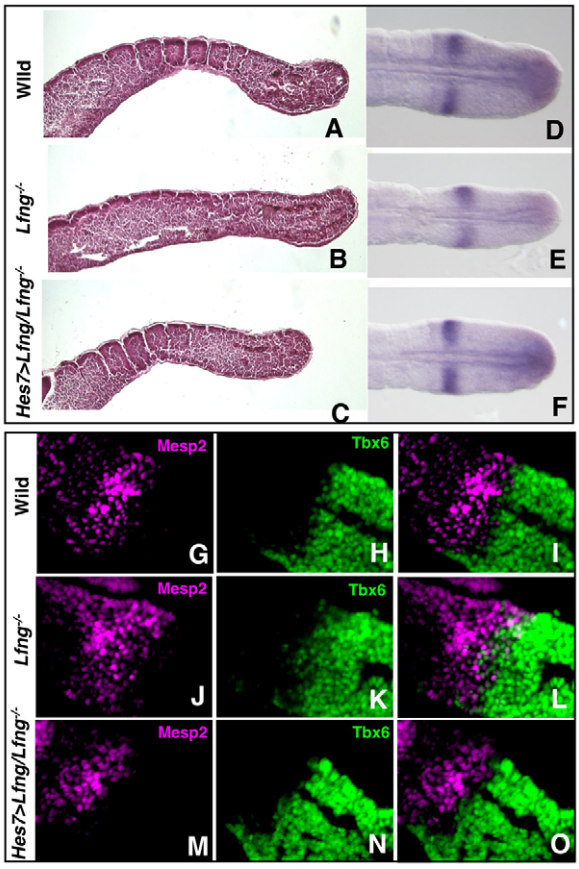

Fig. 3. Exogenous *Lfng* controlled by the *Hes7* promoter completely rescues the boundary formation defect in the *Lfng*$^{-/-}$ mice. The segmental morphologies (**A-C**), the *EphA4* expression pattern (**D-F**) and the relationship between Mesp2 and Tbx6 in Phase II (**G-O**) were compared among wild-type (A,D,G-I), *Lfng*$^{-/-}$ (B,E,J-L) and *Hes7>Lfng/Lfng*$^{-/-}$ (C,F,M-O) using E11.5 embryonic tail regions. Single channels for Mesp2 (G,J,M) and Tbx6 (H,K,N), and merged images of both (I,L,O), are shown. Expression of the *EphA4* and Tbx6 protein boundary forms a clear border in the wild-type (D, *n*=7; G-I, *n*=4) and *Hes7>Lfng/Lfng*$^{-/-}$ embryos (F, *n*=4; M-O, *n*=4), but this is diffuse or randomized in the *Lfng*$^{-/-}$ embryos (E, *n*=4; J-L, *n*=3).

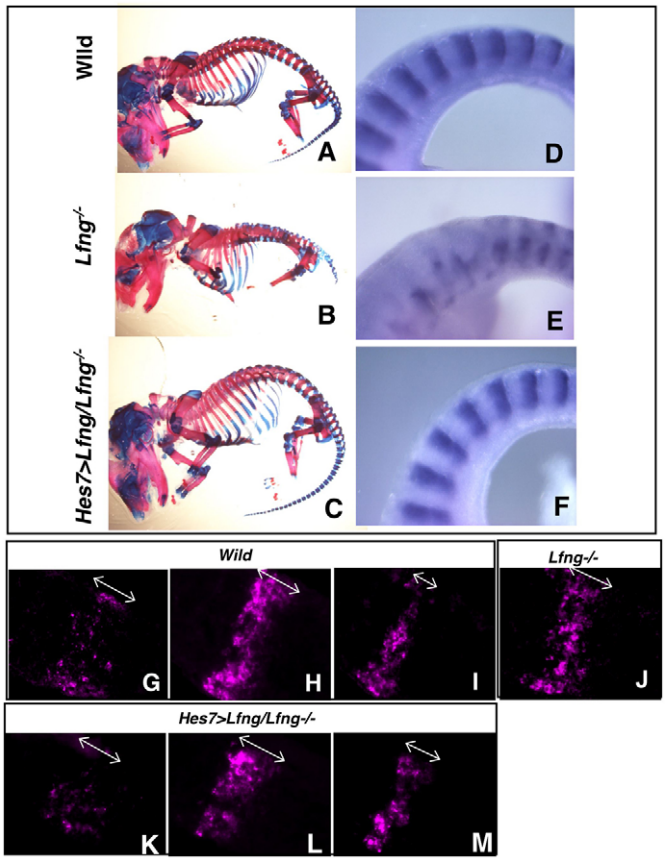

Fig. 4. Exogenous *Lfng* under the control of the *Hes7* promoter completely rescues the R-C patterning defect in the somites of *Lfng*$^{-/-}$ mice. A comparison of the segmental morphologies of skeletal preparations of E17.5 embryos (**A-C**) and the expression pattern of *Uncx4.1*, indicative of R-C patterning within a somite (**D-F**). *Hes7>Lfng/Lfng*$^{-/-}$ mice show a normal skeleton (C, *n*=4) and expression pattern of *Uncx4.1* (F, *n*=3), whereas *Lfng*$^{-/-}$ mice show randomized pattern of skeleton (B) and *Uncx4.1* expression (E). (**G-M**) *Mesp2* transcription states revealed by high resolution in situ hybridization analysis of wild-type embryos for transcriptional initiation (G, *n*=3), active state (H, *n*=5) and rostral localization (I, *n*=3), and *Lfng*-null (J, *n*=11) and *Hes7>Lfng/Lfng*$^{-/-}$ embryos for transcriptional initiation (K, *n*=2), active state (L, *n*=3) and rostral localization (M, *n*=3). Double arrows indicate the length of the *Mesp2* transcription domains.

the anterior PSM is not required for normal R-C polarity patterning. To elucidate this issue further, we focused on the expression of *Mesp2*, which is thought to be the final output signal of the segmentation clock. *Mesp2* is initially expressed over one somite length and then becomes localized in the rostral compartment (Takahashi et al., 2000). This dynamic expression pattern generates a gradient of Mesp2 activity that allows PSM cells to form the R-C pattern within a somite (Takahashi et al., 2003; Takahashi et al., 2000). We therefore next compared the *Mesp2* expression pattern at the cellular level among the wild-type, $Lfng^{-/-}$ and $Hes7{>}Lfng/Lfng^{-/-}$ embryos using high-resolution in situ hybridization. By focusing on the length of the *Mesp2* transcription domain along the A-P axis, we found four distinct patterns in the wild-type embryos: (1) no signal (*n*=4/15); (2) most cells show nuclear dots indicating transcriptional initiation, and the length of the *Mesp2* transcription domain is approximately 11-13 cells (Fig. 4G; *n*=3/15); (3) active stage in which signals can be observed in the cytoplasm in addition to nuclear dots, and the length of *Mesp2* transcription is approximately 10-12 cells, with anterior cells showing stronger signals (Fig. 4H; *n*=5/15); and (4) rostral localization in which the length of the *Mesp2* transcription domain becomes approximately 5-6 cells (Fig. 4I; *n*=3/15). In contrast to wild-type embryos, only one pattern was observed in the *Lfng*-null embryos: signals were observed in the cytoplasm in addition to nuclear dots, the expression levels were randomized for each cells, and the length of the *Mesp2* transcription domain was approximately 9-11 cells (Fig. 4J; *n*=11/11). These results indicate that *Mesp2* expression is always present in the anterior PSM without clear on/off cycles in the *Lfng*-null embryo. In addition, the *Mesp2* expression domain is kept to one somite length and there is no clear localization into the rostral compartment, although cellular or cell cluster-level localization might occur in a salt-and-pepper pattern in the absence of Lfng. Importantly, the *Mesp2* expression pattern was found to show four distinct patterns similar to those in wild-type embryos even in the $Hes7{>}Lfng/Lfng^{-/-}$ embryos, i.e. no signal (1/9), transcriptional initiation (Fig. 4K, *n*=2/9), active stage (Fig. 4L, *n*=3/9) and rostral localization (Fig. 4M; *n*=3/9). Our findings thus indicate that the oscillation of cNICD alone is sufficient to generate the normal *Mesp2* expression pattern and that the anterior PSM-specific regulation of cNICD via Lfng is dispensable for this process.

Modeling of the *Mesp2* expression pattern

To test the validity of our above hypothesis, we performed computer simulations. Our model is based on that previously proposed by Lewis and colleagues, in which the oscillatory waves emanate, travel and eventually cease, as it adopts the notion of maturity, which delays the oscillation cycle towards the anterior as time proceeds (Palmeirim et al., 1997). In this model of Lewis, the cessation of the oscillatory waves triggers periodic gene expression along an anterior-posterior direction that leads to the formation of the somites (Palmeirim et al., 1997). In our current study, we applied the Lewis model to the oscillatory waves of the cNICD and assumed Fgf as a molecular basis for maturity. We further incorporated the regulatory network required for *Mesp2* expression, in which cNICD oscillation and Tbx6 synergistically activate (Yasuhiko et al., 2006; Oginuma et al., 2008), whereas the Fgf gradient suppresses *Mesp2* expression and Tbx6 is degraded downstream of Mesp2 (Fig. 5A). Very surprisingly, this simple simulation successfully mimicked some specific features of dynamic *Mesp2* transcription (red line), not only in terms of on/off cycles but also with regard to temporal changes in the expression pattern (from one somite length to rostral localization) along the anterior-posterior axis (Fig. 5B; see Movie 1 in the supplementary material), similar to that observed in vivo (Fig. 4G-I; see Fig. S3A,B in the supplementary material). In addition, this simulation also reproduced the gradient of Mesp2 activity accumulation (black line), which is similar to the *Mesp2*-β-gal pattern we observed in the $Mesp2^{lacZ/+}$ embryos (see Fig. S3E in the supplementary material).

To test the importance of the cNICD wave for the gradient formation of Mesp2 activity, we examined *Mesp2* expression under constant activity of cNICD in the PSM (Fig. 5C; see Movie 2 in the supplementary material). In this instance, *Mesp2* expression is always observed in the anterior PSM without either clear on/off cycles or localization at the rostral compartment, which is very similar to the in vivo situation of the $Lfng^{-/-}$ embryos (Fig. 4J; see Fig. S3C,D,F in the supplementary material). Interestingly, in our model, neither the formation of the waved pattern of cNICD nor its migration is necessary to establish the gradient of Mesp2 activity because a spatially uniform, but temporally oscillating, Notch signaling activity is sufficient to reproduce this gradient (see Fig. S4 and Movie 3 in the supplementary material). Without a traveling wave, however, the temporal transition of the Mesp2 expression pattern from a one-somite length to a rostral localization was not reproduced (see Fig. S4 and Movie 3 in the supplementary material). We thus speculate that this transition might be important for robust somite formation with a correct R-C polarity and propose that the wave of Notch activity enables PSM cells to establish not only the periodic expression of *Mesp2*, but also their localization into the rostral compartment. Our model therefore provides a new concept that indicates that a progressive oscillating wave of Notch activity is translated into the R-C polarity of a somite through the regulation of the Mesp2 expression pattern.

Anterior PSM-specific *Lfng* cannot rescue the defects in *Mesp2*-null or *Lfng*-null mice

Finally, to further ask the significance of the anterior striped cNICD domain for somite boundary formation, we established a mouse line that reproduces this expression pattern by introducing *Lfng* cDNA at the *Mesp2* locus using embryonic stem cell-mediated homologous recombination (see Fig. S1E in the supplementary material). The resulting heterozygous mice showed no abnormalities and we generated an intercross of $Mesp2^{Lfng/+}$ to yield $Mesp2^{Lfng/Lfng}$. In the $Mesp2^{Lfng/Lfng}$ embryos, cNICD signals were suppressed in the *Lfng*-expressing cells in the anterior PSM (Fig. 6B), as seen in the wild type (Fig. 6A). We further found that some of the cells that did not express *Lfng* maintained cNICD signals, indicating that Lfng suppresses cNICD production in a cell-autonomous manner (Fig. 6D). However, Lfng did not rescue the phenotype of the *Mesp2*-null mice (Fig. 6H-M), indicating that the function of *Lfng* downstream of *Mesp2* is not important.

We next introduced this transgene into the *Lfng*-null genetic background to generate a $Mesp2^{Lfng/+}Lfng^{-/-}$ mouse. The expression levels of *Lfng* in the *Mesp2* locus were found to be low (Fig. 6C,E; see Fig. S5C in the supplementary material), but we did observe downregulation of the cNICD signal in the *Mesp2*-expressing cells (Fig. 6F) in comparison with the *Lfng*-null embryos (Fig. 6G). Furthermore, *Hes5* expression (see Fig. S5D in the supplementary material), a target gene of Notch signaling, was severely downregulated in both the $Mesp2^{Lfng/Lfng}$ and $Mesp2^{Lfng/+}Lfng^{-/-}$ embryos (see Fig. S5F,H in the supplementary material) compared with *Mesp2*- and *Lfng*-null embryos (see Fig. S5E,G in the supplementary material), indicating that *Lfng* under the control of *Mesp2* might effectively suppress Notch signaling. However, we did

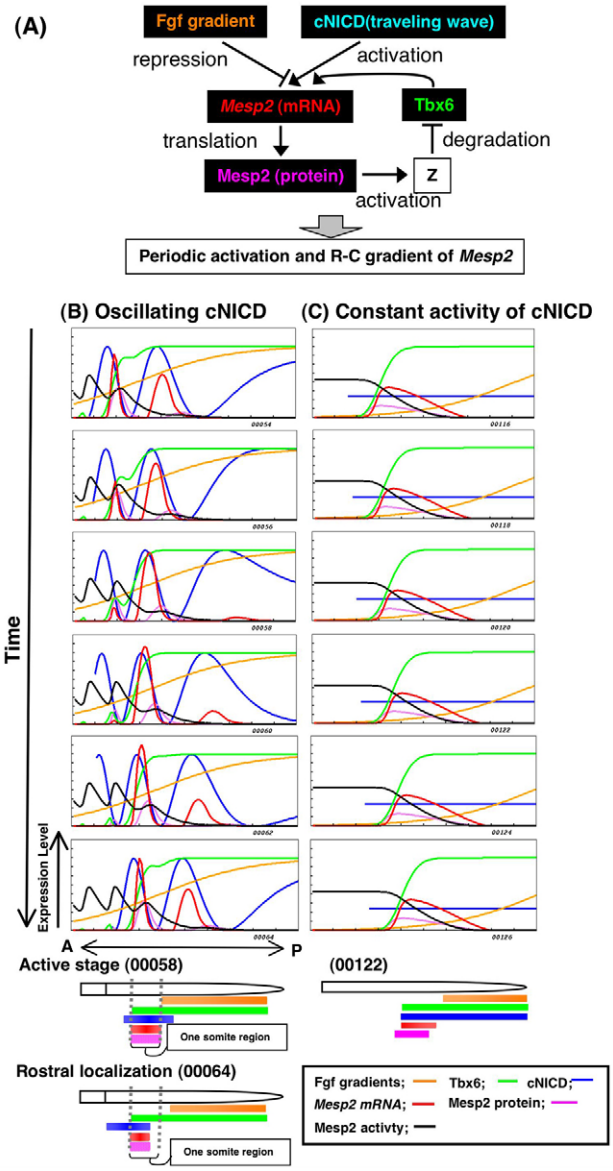

Fig. 5. Model of *Mesp2* expression. (**A**) Schematic representation indicating relationships among *Mesp2* mRNA, Mesp2 protein, Tbx6, cNICD and Fgf signaling, which is used for computer simulation to reproduce the periodic activation and R-C gradient of *Mesp2* expression. z is a hypothetical molecule that functions downstream of Mesp2 and mediates negative-feedback regulation of Tbx6. (**B**,**C**) Expression patterns of *Mesp2*, cNICD and other proteins along the anteroposterior axis predicted in our numerical model. Snapshot images of computer simulations of one cycle of somite formation in the presence (B) or absence (C) of cNICD oscillation are shown. Colored lines indicate levels of cNICD (blue), Fgf8 (orange), *Mesp2* expression (mRNA, red line; protein, pink line) and Tbx6 (green). Mesp2 activity, reflecting the total accumulation of Mesp2 protein, is shown as a tracking line in black. Data sets were taken from Movies 1 (frame 54-64) and 2 (frame 116-126) in the supplementary material, respectively. cNICD (blue) was made to disappear in the panels after one somite is formed, according to experimental observations (Morimoto et al., 2005; Oginuma et al., 2008). Lower diagrams indicate the relationships among these factors at critical time points. Snapshot (00058) corresponds to the transcriptionally active stage of *Mesp2* in which a cNICD wave (blue) reaches the anterior PSM and *Mesp2* (red) is activated in the one-somite region. Snapshot (00064) corresponds to the rostral localization stage, i.e. following the anterior shift of the cNICD wave, the *Mesp2* expression domain also shifts to the rostral region, generating a gradient of Mesp2 activity (black). As the level of cNICD is constant in the *Lfng*-null situation [corresponding to snapshot (00112)], *Mesp2* expression (red) does not show a dynamic pattern and regresses posteriorly.

not detect any significant rescue of the segmental morphology in the developing embryos or of the vertebral morphology at any level along the anteroposterior axis in the $Mesp2^{Lfng/+}Lfng^{-/-}$ mice compared with the *Lfng*-null mouse (Fig. 6N-Q; see Fig. S6 in the supplementary material). These results further confirmed that the suppression of cNICD signaling by stabilized Lfng is not sufficient for normal somitogenesis to occur.

DISCUSSION

The requirement for Notch signaling during mouse somitogenesis

In our current study, we reveal that the cNICD on/off state is not required for somite boundary formation during somitogenesis in the mouse. Consistent with this, recent studies in zebrafish embryos suggest that the function of Notch signaling is only to synchronize the oscillations among PSM cells, and that this pathway has no other function during segmentation (Riedel-Kruse et al., 2007; Horikawa et al., 2006; Ozbudak and Lewis, 2008). However, we propose from our current data that Notch signaling has a crucial function also as an output of the segmentation clock during mouse development. This contention is supported by earlier evidence that *Mesp2* expression is severely downregulated in the absence of Notch signaling (Barrantes et al., 1999; Takahashi et al., 2000). Moreover, it has been shown that constitutive activation of Notch signaling in the paraxial mesoderm induces *Mesp2* transcription without clear on/off cycles (Feller et al., 2008) and it is also evident from other reports that Notch signaling is crucial for the establishment of R-C patterning of somites in the mouse (Takahashi et al., 2000; Takahashi et al., 2003; Feller et al., 2008). These results together suggest that the function of Notch signaling is not only to synchronize oscillations but that Notch acts also as an important output signal of the segmentation clock, at least in mouse somitogenesis. We thus speculate that Notch signaling is a key factor that mediates the transduction of clock activities into the morphological segmental pattern by regulating *Mesp2* expression. However, it is known that several oscillating components in Notch, Wnt and Fgf signaling pathways are coordinated to generate the segmentation clock network in mice. Hence, *Mesp2* transcription might not be regulated by Notch signaling alone and several pathways might govern the spatiotemporal pattern of *Mesp2* expression. The coordination of these complex networks might well be fundamental to normal somitogenesis.

A new model for the establishment of R-C polarity during somitogenesis

Based on our present findings, we propose a new function for oscillating Notch signaling, which is translated into the R-C polarity of a somite via the regulation of *Mesp2* expression in the anterior PSM. Previous models have proposed that the establishment of R-C polarity requires cell-cell communication (Takahashi et al., 2003; Dale and Pourquie, 2000), whereas we propose a model in which a

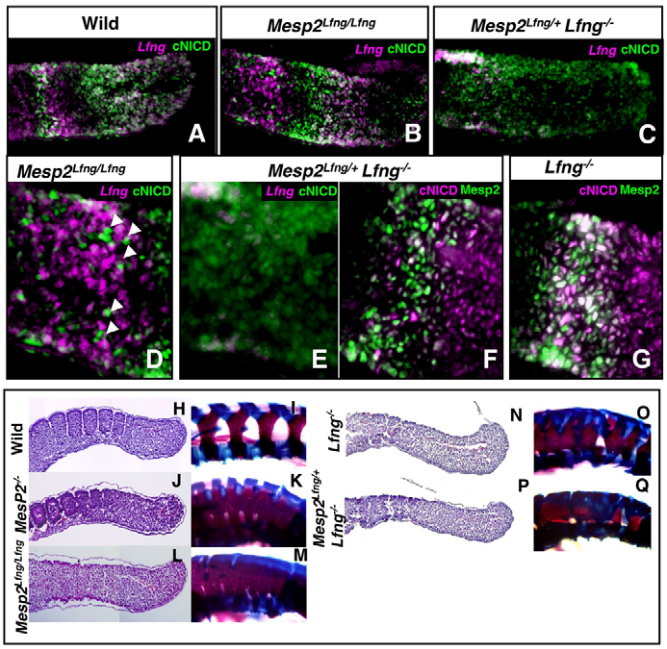

Fig. 6. Exogenous *Lfng* under the control of the *Mesp2* promoter does not rescue the phenotype of the *Mesp2*$^{-/-}$ or *Lfng*$^{-/-}$ mouse. (**A-G**) Sections of E11.5 embryos double stained for *Lfng* mRNA and cNICD (A-E) or for Mesp2 and cNICD (F,G). Higher magnification images of B and C are shown in D and E, respectively. In the *Mesp2*$^{Lfng/Lfng}$ embryo, cNICD formation (B,D, *n*=3) is suppressed in the anterior PSM. The arrowheads in D indicate *Lfng* non-expressing cells that maintain cNICD formation cell-autonomously. In the *Mesp2*$^{Lfng/+}$*Lfng*$^{-/-}$ embryos, cNICD (F, *n*=5) is effectively suppressed in the Mesp2-expressing cells compared with *Lfng*-null embryos (G, *n*=6). (**H-Q**) Comparison of the segmental morphologies in the E11.5 embryonic tail region (H,J,L,N,P) and E17.5 vertebral region (I,K,M,O,Q) among the different genotypes indicated. Neither the *Mesp2*$^{Lfng/Lfng}$ (L,M) nor *Mesp2*$^{Lfng/+}$*Lfng*$^{-/-}$ (P,Q) mice show any recovery of the *Mesp2*$^{-/-}$ (J,K) or *Lfng*$^{-/-}$ (N,O) phenotypes. Number of samples: H, *n*=4; I, *n*=6; J, *n*=3; K, *n*=4; L, *n*=3; M, *n*=6; N, *n*=3; O, *n*=6; P, *n*=3; Q, *n*=7.

cell-autonomous mechanism utilizes Notch signaling oscillation in the posterior PSM. This notion is further supported by computer simulations, in which we found that an appropriate translation of spatiotemporal information provided by the traveling wave of cNICD is sufficient to create the dynamic *Mesp2* expression pattern, i.e. on/off cycles and rostral localization (Fig. 5B; see Movie 1 in the supplementary material). In these simulation experiments, the generation of the traveling wave was based on the earlier work of Lewis (Palmeirim et al., 1997), and the translation of the wave information into *Mesp2* expression was modeled on the gene network that we elucidated previously (Oginuma et al., 2008; Yasuhiko et al., 2006). In the model, the cNICD wave, an activator of *Mesp2*, travels from the posterior to the anterior, whereas the levels of Fgf, a repressor of *Mesp2*, are higher toward the posterior. Consequently, as a single wave passes through a nascent somite, the net transcriptional activation of *Mesp2*, which reflects the amount of cNICD subtracted by the amount of Fgf, is higher toward the rostral part of the presumptive somite. The resulting gradient of Mesp2 activity might thus allow PSM cells to establish a rostral identity and the segmental border. Hence, this is the first model to demonstrate that R-C polarity in the somite is generated as a direct output of the segmentation clock.

The repression of Tbx6, an activator of *Mesp2*, downstream of Mesp2 is another important component in our model. This regulatory module prevents *Mesp2* expression after one traveling wave of cNICD has passed, and thus fixes the R-C gradient pattern of Mesp2. The next wave of Notch signaling cannot affect the Mesp2 pattern created by the former wave. To reproduce the intensive degradation of Tbx6 at anterior regions, we had to adjust the parameters for Tbx6 degradation. We did not need to change any of the other standard parameters we initially chose, suggesting that the qualitative features of the model are not so sensitive to the quantitative values of the parameters. In our simulation analysis, however, we did not reproduce the sharp anterior boundaries of Tbx6 and Mesp2 accumulation (green and black lines, respectively, in Fig. 5B; see Movie 1 in the supplementary material) that have been observed in vivo. To create a sharp boundary of Tbx6 and Mesp2, which should be required to create a fine segmentation boundary, further adjustment of the parameters or another mechanism might be required. In this regard, the next important challenge will be to investigate the molecular basis of the sharpening expression boundaries of Tbx6 and Mesp2, and ultimately to understand how analog inputs (such as sequential wave patterns of oscillation) are converted into digital outputs (such as the square-like stair patterns of the segmental border).

Functions of Lfng in the posterior and anterior PSM during mouse somitogenesis

We also demonstrate from our present data that the oscillatory expression of *Lfng* is both required and sufficient for normal somitogenesis. However, this result will probably be viewed somewhat controversially given the recent findings that have underscored the significance of Lfng expression in the anterior PSM during this process, at least after E10.5 (Shifley et al., 2008; Stauber et al., 2009). The authors of these reports produced transgenic mice harboring *Lfng* expression without oscillation. Their data indicate that cNICD oscillation is disrupted, but that normal segmented somites form, after E10.5 and they concluded that oscillating *Lfng* expression is required only for early stage, but not later stage, somitogenesis (Shifley et al., 2008; Stauber et al., 2009). We wish therefore to discuss some possible explanations for the discrepancies between our current findings and these previous experimental results.

One possibility is that the common expression profiles between our *Hes7>Lfng* mouse and the mice studied in previous reports is important. We demonstrate here that *Hes7* and *Lfng* expression manifest a waved pattern within the Tbx6 expression domain, which includes a part of the anterior PSM. Therefore, in our *Hes7>Lfng* mouse, oscillating *Lfng* expression also exists in the anterior PSM, but not as a stabilized pattern. We suspect that the transgenic mice analyzed in previous reports lack oscillating *Lfng* expression in the posterior PSM but the oscillation might exist in the anterior PSM as well, and thus we speculate that the oscillating *Lfng* expression in the posterior PSM is not required after E10.5, but that in the anterior PSM might be sufficient for normal somitogenesis. Another possibility is that the slightly oscillating expression reported previously might be responsible for the rescue event. Previous studies have shown that two distinct enhancers are involved in the oscillatory expression of *Lfng*, one of which is disrupted in the mouse reported by Shifley et al. (Shifley et al., 2008), and a slight cyclic expression of *Lfng* exists in the mouse generated by Stauber et al. (Stauber et al., 2009). Hence, one possible interpretation for these discrepancies is that the slight cyclic expression of *Lfng* might be sufficient for normal development in the enhancer-specific

knockout mouse after E10.5 somitogenesis, but not prior to E10.5. It is reasonable to assume that the requirement of Notch clock oscillation by *Lfng* changes during somitogenesis and is lesser at later stages, as now suggested by a number of studies (Shifley et al., 2008; Stauber et al., 2009).

Acknowledgements
We thank Ryoichiro Kageyama (Kyoto University) for providing the *Hes7* promoter and enhancer cassette, Aya Satoh, Nobuo Sasaki and Yusuke Okubo (National Institute of Genetics) for animal care and the preparation of embryo samples and Mariko Ikumi, Eriko Ikeno and Shinobu Watanabe (National Institute of Health Sciences) for technical assistance. This work was supported in part by Grants-in-Aid for Scientific Research on Priority Areas, Dynamics of Extracellular Environments, and by the National BioResource Project from the Ministry of Education, Culture, Sports, Science and Technology, Japan.

Competing interests statement
The authors declare no competing financial interests.

Supplementary material
Supplementary material for this article is available at
http://dev.biologists.org/lookup/suppl/doi:10.1242/dev.044545/-/DC1

References
Aulehla, A. and Johnson, R. L. (1999). Dynamic expression of lunatic fringe suggests a link between notch signaling and an autonomous cellular oscillator driving somite segmentation. *Dev. Biol.* **207**, 49-61.
Aulehla, A., Wehrle, C., Brand-Saberi, B., Kemler, R., Gossler, A., Kanzler, B. and Herrmann, B. G. (2003). Wnt3a plays a major role in the segmentation clock controlling somitogenesis. *Dev. Cell* **4**, 395-406.
Aulehla, A., Wiegraebe, W., Baubet, V., Wahl, M. B., Deng, C., Taketo, M., Lewandoski, M. and Pourquie, O. (2008). A beta-catenin gradient links the clock and wavefront systems in mouse embryo segmentation. *Nat. Cell Biol.* **10**, 186-193.
Barrantes, I. B., Elia, A. J., Wunsch, K., Hrabe de Angelis, M. H., Mak, T. W., Rossant, J., Conlon, R. A., Gossler, A. and de la Pompa, J. L. (1999). Interaction between Notch signalling and Lunatic fringe during somite boundary formation in the mouse. *Curr. Biol.* **9**, 470-480.
Bessho, Y., Hirata, H., Masamizu, Y. and Kageyama, R. (2003). Periodic repression by the bHLH factor Hes7 is an essential mechanism for the somite segmentation clock. *Genes Dev.* **17**, 1451-1456.
Cole, S. E., Levorse, J. M., Tilghman, S. M. and Vogt, T. F. (2002). Clock regulatory elements control cyclic expression of Lunatic fringe during somitogenesis. *Dev. Cell* **3**, 75-84.
Dale, K. J. and Pourquie, O. (2000). A clock-work somite. *BioEssays* **22**, 72-83.
Delfini, M. C., Dubrulle, J., Malapert, P., Chal, J. and Pourquie, O. (2005). Control of the segmentation process by graded MAPK/ERK activation in the chick embryo. *Proc. Natl. Acad. Sci. USA* **102**, 11343-11348.
Dequeant, M. L. and Pourquie, O. (2008). Segmental patterning of the vertebrate embryonic axis. *Nat. Rev. Genet.* **9**, 370-382.
Dequeant, M. L., Glynn, E., Gaudenz, K., Wahl, M., Chen, J., Mushegian, A. and Pourquie, O. (2006). A complex oscillating network of signaling genes underlies the mouse segmentation clock. *Science* **314**, 1595-1598.
Evrard, Y. A., Lun, Y., Aulehla, A., Gan, L. and Johnson, R. L. (1998). lunatic fringe is an essential mediator of somite segmentation and patterning. *Nature* **394**, 377-381.
Feller, J., Schneider, A., Schuster-Gossler, K. and Gossler, A. (2008). Noncyclic Notch activity in the presomitic mesoderm demonstrates uncoupling of somite compartmentalization and boundary formation. *Genes Dev.* **22**, 2166-2171.
Horikawa, K., Ishimatsu, K., Yoshimoto, E., Kondo, S. and Takeda, H. (2006). Noise-resistant and synchronized oscillation of the segmentation clock. *Nature* **441**, 719-723.
Lewis, J. (2003). Autoinhibition with transcriptional delay: a simple mechanism for the zebrafish somitogenesis oscillator. *Curr. Biol.* **13**, 1398-1408.
McGrew, M. J., Dale, J. K., Fraboulet, S. and Pourquie, O. (1998). The lunatic fringe gene is a target of the molecular clock linked to somite segmentation in avian embryos. *Curr. Biol.* **8**, 979-982.
Morales, A. V., Yasuda, Y. and Ish-Horowicz, D. (2002). Periodic Lunatic fringe expression is controlled during segmentation by a cyclic transcriptional enhancer responsive to notch signaling. *Dev. Cell* **3**, 63-74.
Morimoto, M., Takahashi, Y., Endo, M. and Saga, Y. (2005). The Mesp2 transcription factor establishes segmental borders by suppressing Notch activity. *Nature* **435**, 354-359.
Nakajima, Y., Morimoto, M., Takahashi, Y., Koseki, H. and Saga, Y. (2006). Identification of Epha4 enhancer required for segmental expression and the regulation by Mesp2. *Development* **133**, 2517-2525.
Niwa, Y., Masamizu, Y., Liu, T., Nakayama, R., Deng, C. X. and Kageyama, R. (2007). The initiation and propagation of Hes7 oscillation are cooperatively regulated by Fgf and notch signaling in the somite segmentation clock. *Dev. Cell* **13**, 298-304.
Oginuma, M., Niwa, Y., Chapman, D. L. and Saga, Y. (2008). Mesp2 and Tbx6 cooperatively create periodic patterns coupled with the clock machinery during mouse somitogenesis. *Development* **135**, 2555-2562.
Ozbudak, E. M. and Lewis, J. (2008). Notch signalling synchronizes the zebrafish segmentation clock but is not needed to create somite boundaries. *PLoS Genet.* **4**, e15.
Palmeirim, I., Henrique, D., Ish-Horowicz, D. and Pourquie, O. (1997). Avian hairy gene expression identifies a molecular clock linked to vertebrate segmentation and somitogenesis. *Cell* **91**, 639-648.
Riedel-Kruse, I. H., Muller, C. and Oates, A. C. (2007). Synchrony dynamics during initiation, failure, and rescue of the segmentation clock. *Science* **317**, 1911-1915.
Sakai, K. and Miyazaki, J. (1997). A transgenic mouse line that retains Cre recombinase activity in mature oocytes irrespective of the cre transgene transmission. *Biochem. Biophys. Res. Commun.* **237**, 318-324.
Shifley, E. T., Vanhorn, K. M., Perez-Balaguer, A., Franklin, J. D., Weinstein, M. and Cole, S. E. (2008). Oscillatory lunatic fringe activity is crucial for segmentation of the anterior but not posterior skeleton. *Development* **135**, 899-908.
Stauber, M., Sachidanandan, C., Morgenstern, C. and Ish-Horowicz, D. (2009). Differential axial requirements for lunatic fringe and Hes7 transcription during mouse somitogenesis. *PLoS One* **4**, e7996.
Takahashi, Y., Koizumi, K., Takagi, A., Kitajima, S., Inoue, T., Koseki, H. and Saga, Y. (2000). Mesp2 initiates somite segmentation through the Notch signalling pathway. *Nat. Genet.* **25**, 390-396.
Takahashi, Y., Inoue, T., Gossler, A. and Saga, Y. (2003). Feedback loops comprising Dll1, Dll3 and Mesp2, and differential involvement of Psen1 are essential for rostrocaudal patterning of somites. *Development* **130**, 4259-4268.
Takahashi, Y., Yasuhiko, Y., Kitajima, S., Kanno, J. and Saga, Y. (2007). Appropriate suppression of Notch signaling by Mesp factors is essential for stripe pattern formation leading to segment boundary formation. *Dev. Biol.* **304**, 593-603.
Wahl, M. B., Deng, C., Lewandoski, M. and Pourquie, O. (2007). FGF signaling acts upstream of the NOTCH and WNT signaling pathways to control segmentation clock oscillations in mouse somitogenesis. *Development* **134**, 4033-4041.
Watanabe, T., Sato, Y., Saito, D., Tadokoro, R. and Takahashi, Y. (2009). EphrinB2 coordinates the formation of a morphological boundary and cell epithelialization during somite segmentation. *Proc. Natl. Acad. Sci. USA* **106**, 7467-7472.
Yasuhiko, Y., Haraguchi, S., Kitajima, S., Takahashi, Y., Kanno, J. and Saga, Y. (2006). Tbx6-mediated Notch signaling controls somite-specific Mesp2 expression. *Proc. Natl. Acad. Sci. USA* **103**, 3651-3656.
Zhang, N. and Gridley, T. (1998). Defects in somite formation in lunatic fringe-deficient mice. *Nature* **394**, 374-377.